Available online at www.sciencedirect.com
SCIENCE DIRECT
Polymer 47 (2006) 4564–4570
polymer
www.elsevier.com/locate/polymer

Improving the physical properties of PEA/PMMA blends by the uniform dispersion of clay platelets

Yijin Xu [a], William J. Brittain [a,*], Richard A. Vaia [b], Gary Price [c]

[a] Department of Polymer Science, The University of Akron, Akron, OH 44325-3909, USA
[b] Air Force Research Laboratory, Materials and Manufacturing Directorate, WPAFB, OH 45433, USA
[c] The University of Dayton Research Institute, Dayton, OH 45469, USA

Received 26 October 2005; received in revised form 19 March 2006; accepted 28 March 2006
Available online 18 May 2006

Abstract

Poly(ethyl acrylate) (PEA)/poly(methyl methacrylate) (PMMA) emulsion blends that were combined with unmodified montmorillionite (MMT) to improve the physical properties via nanocomposite formation. We prepared a cationic PEA/PMMA latex and used a heterocoagulation process to create a homogeneous dispersion of the clay platelets in the matrix. The cationic PEA/PMMA emulsion blends were prepared using a cationic initiator in the presence of free surfactant, cetyl trimethylammonium bromide (CTABr), followed by mixing with an aqueous slurry of MMT. The PEA/PMMA–MMT nanocomposites could be processed at low temperatures. Low temperature processing prevented the commonly observed discoloration associated with many thermoplastic nanocomposites. DSC, SAXS, TEM and AFM were used to study the dispersion of MMT and morphology of PEA/PMMA–MMT nanocomposites. Tensile stress, elongation at break and Young's modulus demonstrated a significant reinforcing effect of clay.

Keywords: Elastomers; Nanocomposites; Montmorillonite (MMT)

1. Introduction

Mayes and co-workers have developed a new type of polymer system with low processing temperatures that they have entitled baroplastics [1]. Baroplastics can be block copolymer elastomers, core–shell polymers or simple polymer blends that contain a plastic phase and a rubber phase. They undergo a pressure-induced transition from the ordered state (solid like) to a disordered state (liquid like) [2–5]. One advantage of baroplastics is low temperature processing that avoids the degradation of polymers and additives while maintaining a reasonable plastic performance and recyclability. In this paper, we report the preparation of PEA/PMMA–clay nanocomposites by heterocoagulation, that has some characteristics of baroplastics such as low temperature processing and pressure-induced miscibility, and report on their low temperature processability, morphology and mechanical properties.

Because of the molecular level interactions, nanoscale dimensions, and high aspect ratio of the clay silicates, some polymer-layered silicate nanocomposites (PLSNs) have shown improvements in mechanical, electrical, optical, barrier, and thermal properties when compared with micro- and macrocomposite counterparts [6]. One experimental challenge of PLSNs is the thermal decomposition of the clay organic modifier at processing temperatures that lead to discoloration and decomposition of the clay modifier [7]. Thermogravimetric analysis (TGA) has indicated that standard alkyl ammonium modifiers can decompose at 180 °C under non-oxidative environments [8,9]. This temperature is usually lower than typical processing temperatures used to prepare and/or process PLSNs. Some research groups have focused on clay modifiers with higher decomposition temperatures such as imidazolium and phosphonium groups [10–14].

Our group has reported the use of a heterocoagulation method to prepare PLSNs that involves the following steps: (1) preparation of a cationic polymer latex by a conventional emulsion polymerization, (2) mixing the cationic polymer latex with an aqueous slurry of unmodified clay, and (3) heterocoagulation to produce an exfoliated nanocomposite [15–17]. This process is simple and environmentally friendly because an emulsion polymerization can be used to make

* Corresponding author. Tel.: +1 330 972 5147; fax: +1 330 972 5290.
E-mail address: wjbritt@uakron.edu (W.J. Brittain).

0032-3861/$ - see front matter © 2006 Elsevier Ltd. All rights reserved.
doi:10.1016/j.polymer.2006.03.108

master batches. Because alkyl ammonium surfactants are used in the emulsion polymerization, we have observed discoloration problems during processing. As an alternative to using the more thermally stable imdazolium/phosphonium surfactants, we propose to exploit the low processing temperatures of baroplastics to avoid the discoloration and decomposition problems.

2. Experimental section

2.1. Materials

Montmorillonite (MMT, GelWhite GP®) was provided by Southern Clay Products. 2,2′-Azobis(2-amidinopropane) dihydrochloride (V-50), provided by Wako Pure Chemical Industries Ltd, was used without further purification. Cetyltrimethylammonium bromide (CTABr) was obtained from Aldrich and used as received. Methyl methacrylate (MMA) and ethyl acrylate from Aldrich were purified by passage through a basic alumina oxide. Deionized water was used in all the experiments.

2.2. Instrumentation

Small angle X-ray scattering (SAXS) results were collected on an molecular metrology SAXS camera with a double focusing design using a bent Au-coated mirror to focus in the vertical plane and a bent, asymmetric Si (111) monochromator to focus in the horizontal plane. The detector was a two-dimensional multi-wire detector from molecular metrology and the sample to detector distance was 127.6 cm. The X-ray source was a Rigaku R-200 rotating anode generator with a copper target and a focus of a 0.3×0.3 mm^2 cathode assembly. The generator was run at 45 kV and 70 ma for a 30 min exposure time. Transmission electron microscopy (TEM) experiments were performed on a Philips CM200 LaB6 TEM operating at 200 kV accelerating voltage. The samples were cryo-ultramicrotomed on an RMC Power-Tome XL utilizing the CR-X cryosectioning attachment at −25 °C to give ~75–100 nm thick sections, which were transferred onto standard 400 mesh hexagonal Cu TEM grids. An atomic force microscope (AFM, Veeco Digital Instrument Nanoscope IIIA) was used to map the distribution of clay platelets, hard PMMA particles and soft PEA phase in the nanocomposites. The specimen for AFM experiments was ultra-microtomed with a diamond knife on a Reichert Ultracuts (Leica) microtome at −30 °C to give a smooth surface. Tapping mode was used to obtain phase images for the nanocomposites at ambient temperature. Thermogravimetric analysis (TGA) was performed on a Hi-Res TGA 2950 thermograimetic analyzer (TA instruments) with a temperature range of 25–800 °C at a heating rate of 20 °C/min. Differential scanning calorimetry (DSC) experiments were run on a TA Instruments DSC 2920 Modulated DSC under a nitrogen atmosphere. A sealed sample was heated from −50 to 150 °C at a rate of 10 °C/min; after the first run it was removed and quickly cooled to room temperature. We report the results from the second run in this paper. Tensile tests were performed according to ASTM D412 on tensile specimens using an Instron model 5567. Young's modulus was determined on a Rheometric Scientific TM (DMTA V) in a static tensile configuration at 24 °C under a nitrogen atmosphere.

2.3. Preparation of cationic PMMA/PEA latex blends

The emulsion polymerization of MMA and EA are the same as reported elsewhere [16,17]. A typical process for the preparation of PMMA/PEA latex blends is as follows. Into a four-necked 1 L Pyrex reaction kettle, which was equipped with a mechanical stirrer, argon inlet, thermometer and refluxing condenser, were placed 400 mL of deionized water, 82 g of purified EA, 0.8 g of CTABr, and 1.2 g of V-50. Into another four-necked 500 mL Pyrex reaction kettle, which was equipped with a mechanical stirrer, argon inlet, thermometer and refluxing condenser, were placed 375 mL of deionized water, 75 mL of purified MMA, 0.4 g of CTABr, and 1.1 g of V-50. The reaction contents were purged with argon for 45 min while stirring at 300 rpm followed by heating at 65 °C. After 3 h, the PMMA emulsion was transferred to the PEA emulsion, and the mixture was heated at 70 °C for 90 min and 75 °C for another 3 h before the polymerization was stopped by cooling to room temperature. A sample of the latex was taken out for the determination of monomer conversion by gravimetry.

2.4. Heterocoagulation

A 1% (w/w) clay slurry was prepared by suspending native MMT clay in water with rigorous stirring overnight. A predetermined amount of cationic latex and clay slurry were mixed together in a beaker while stirring. The mixture was stirred for 2 h and then aqueous magnesium sulfate solution was added into the mixture for de-emulsification. After filtering and washing with distilled water, the precipitate was collected and dried at room temperature in vacuo until constant weight.

2.5. Sample preparation by compression molding

For tensile and Young's modulus testing, the dry samples were compression molded. A known amount of nanocomposite powder was pressed at 15 MPa at 40 °C for 5 min; then the mold was removed and cooled with water. For remolding, the tested specimens were shredded into small pieces and remolded under the same conditions. The samples for TGA and DSC measurements were taken from the specimens after tensile testing. The results for Young's modulus, tensile stress, TGA, DSC, TEM and AFM measurements were determined using samples that had been molded twice.

3. Results and discussion

3.1. Discoloration and pressure induced miscibility

The published benefits of materials like baroplastics is low temperature processing, which limits the thermally-induced

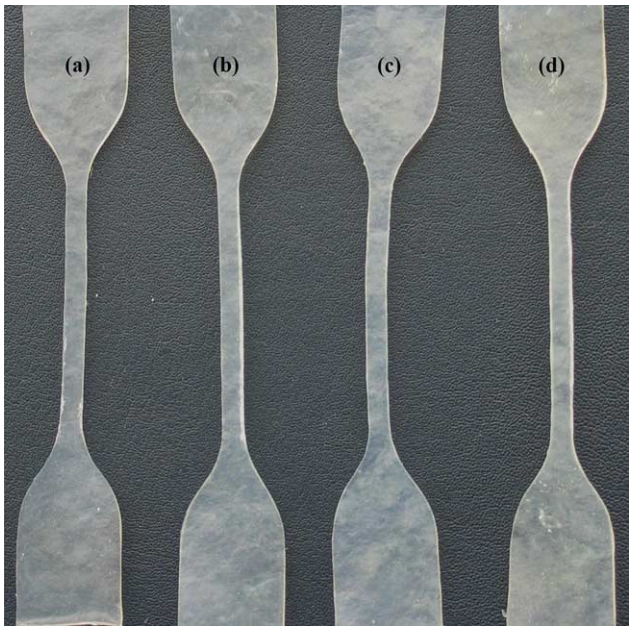

Fig. 1. Photos of pure PEA/PMMA blends and PEA/PMMA–MMT nanocomposites of different MMT loading after twice processed at 40 °C under a pressure of 15 MPa: (a) pure PEA/PMMA blends, (b), (c), and (d) are the nanocomposites of 0.51, 1.35 and 1.59% MMT, respectively.

degradation of polymers and additives, decreases the possibility of discoloration of polymer materials during processing and offer the potential for recyclability. These benefits should be particularly useful for PLSNs. Fig. 1 displays photos of the PEA/PMMA–MMT nanocomposites after double processing at 40 °C and under a pressure of 15 MPa. The pictures clearly demonstrate no discoloration.

We studied the thermal transitions of pure PEA/PMMA blends and PEA/PMMA–MMT nanocomposites before and after molding twice at 40 °C at 15 MPa via DSC (Fig. 2). We observed that the glass transition of PEA remained unchanged, the PMMA transition became weaker, and a new transition appeared around 40–50 °C. In another paper [17], we also observed that in PEA–MMT nanocomposites that there is a negligible change in the glass transition temperature. We speculate that the molding process alters the phase behavior from co-continuous to a continuous PEA phase (which can been seen in Fig. 6); the new transition around 40–50 °C is probably due to the increased interfacial region created by pressure-induced miscibility. This could not be from mold-induced strain because the data were taken from the second run of DSC experiments. This result is consistent with results from Mayes and co-workers [18]. However, it is not consistent with Cowie and co-workers [19], because our PEA/PMMA blends possess number average molecular weights higher than 200,000 g/mol and polydispersities were approximately 2.0. Cowie and co-workers reported that PEA/PMMA miscibility was only observed for lower molecular polymers; however, their work did involve polymers with significantly lower polydispersities. We plan more research to resolve this contradiction.

3.2. Morphology characterization

Fig. 3 shows the SAXS results of PEA/PMMA blends and their composites up to $2\theta = 10°$. There is a peak corresponding to 3.47 nm that appeared in all nanocomposites, which suggests the existence of some intercalated structures. At higher MMT

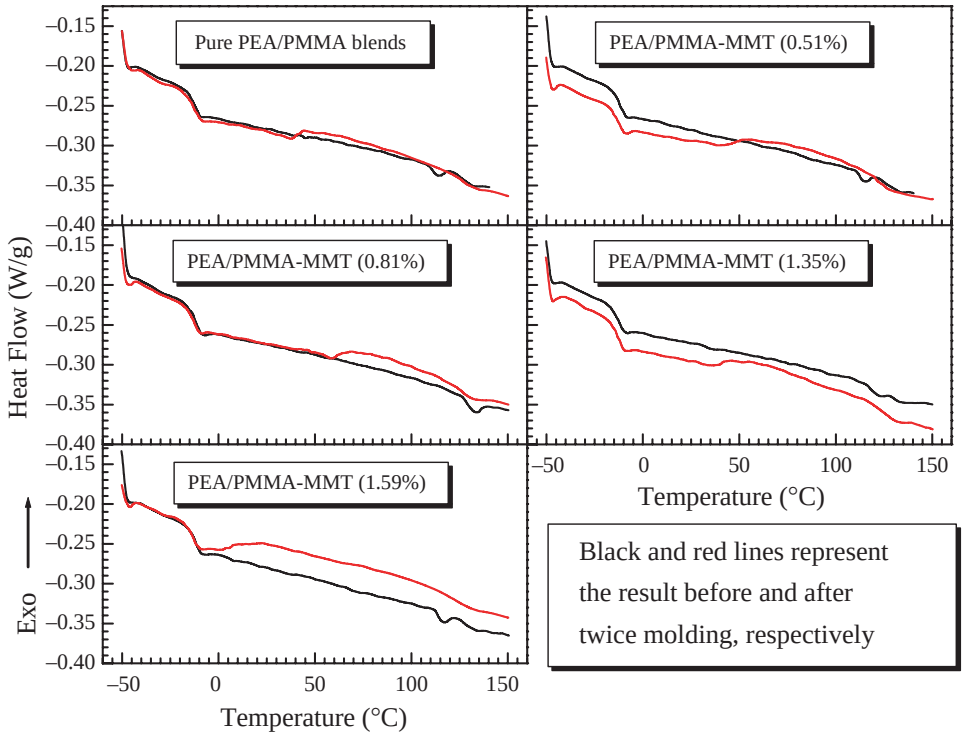

Fig. 2. DSC traces of PEA/PMMA and their MMT nanocomposites before and after twice molding at 40 °C under a pressure of 15 MPa.

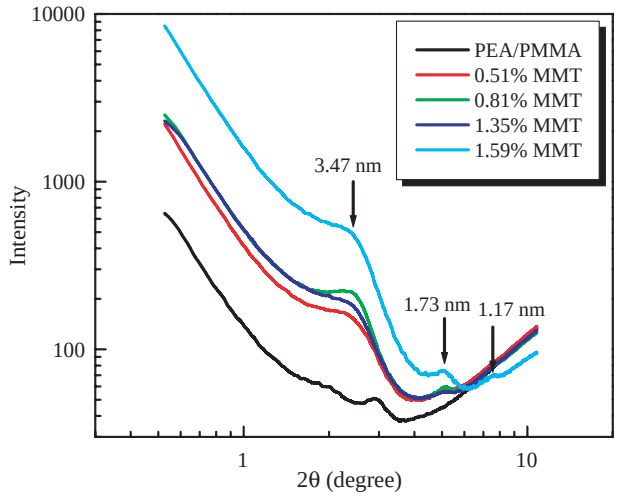

Fig. 3. SAXS results of PEA/PMMA blends and PEA/PMMA–MMT nanocomposites, the values before 'MMT' are clay loadings.

loadings, there is another peak centered at 1.73 nm while we observed a peak corresponding to a 1.17 gallery spacing for a PEA/PMMA–MMT nanocomposite containing 1.59% MMT. This suggests some ordered structures in the nanocomposites. Together with the SAXS pattern and Azimuthl degree shown in Fig. 4, we have concluded that some clay platelets are parallel with the surface of the molded specimen, because all these experiments were performed with the X-ray beam parallel to the specimen surface.

To further check the dispersion and alignment of clay platelets in the polymer blends matrix, TEM experiments were performed on these specimens. Fig. 5 shows the low and high magnification TEM images of the PEA/PMMA–MMT nanocomposite with a 1.59% MMT loading. Fig. 5(a) demonstrates a homogeneous dispersion of the clay platelets. In Fig. 5(b), we observed 2–3 layer stacks of clay platelets consistent with WAXD peaks centered at 1.73 and 1.17 nm. We think the larger particles (which we have denoted with circles in the images) are the magnesium sulfate that was used in the de-emulsification.

Because we processed the MMT nanocomposite with PEA/PMMA at 40 °C, we believe that the hard PMMA spheres preserved their original particle structure. There are few reports about the compatibilization properties of clay in polymer blend systems [20–22]. Fig. 6 is a tapping mode AFM image of a PEA/PMMA–MMT nanocomposite (1.59% MMT). From this image, we speculate that: (1) the PMMA particles preserve their spherical structure; (2) the clay platelets mix with the both rubber and plastic phases; (3) the clay platelets are oriented in the polymer blend; and (4) there appears to be an interaction between clay platelets and cationic latex particles that is consistent our previous results [16].

3.3. Mechanical and thermal properties

The incorporation of clay platelets into a polymer matrix usually increases the modulus and makes materials more brittle. Fig. 7 shows the effect of MMT on the tensile stress and elongation at break. As the clay loading was increased from 0 to 1.59%, the tensile stress increased by 23%, which is an unusually large increase. The elongation at break effect was modest because we only observed a change from 600 to 700%. Fig. 8 displays the effect of MMT loading on the stress–strain relationship. With increasing clay loading, the increase of stress at higher strain is more significant. Fig. 9 shows the result of the Young's modulus with respect to clay loading. When the clay loading increased from 0 to 1.59%, the Young's modulus increased from 0.24 to 0.54 MPa, corresponding to a 120% increase. To our knowledge, this magnitude of increase has not been previously observed in polymer–clay systems. The probable reason is that it is much easier to increase the modulus of a soft matrix with fillers [23,24]. In our PEA/PMMA–MMT system, there is not chemical crosslinking; therefore, we speculate that the increase in tensile stress and Young's modulus is largely due physical crosslinking that involve the clay platelets (the electrostatic interaction between clay and the rubber phase).

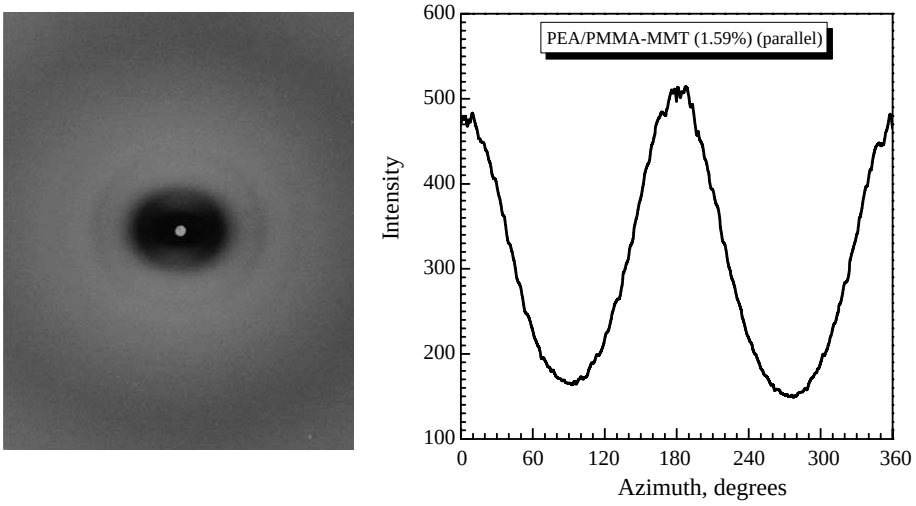

Fig. 4. SAXS diffraction patterns of Azimuth angle for PEA/PMMA–MMT nanocomposite of 1.59% MMT loading.

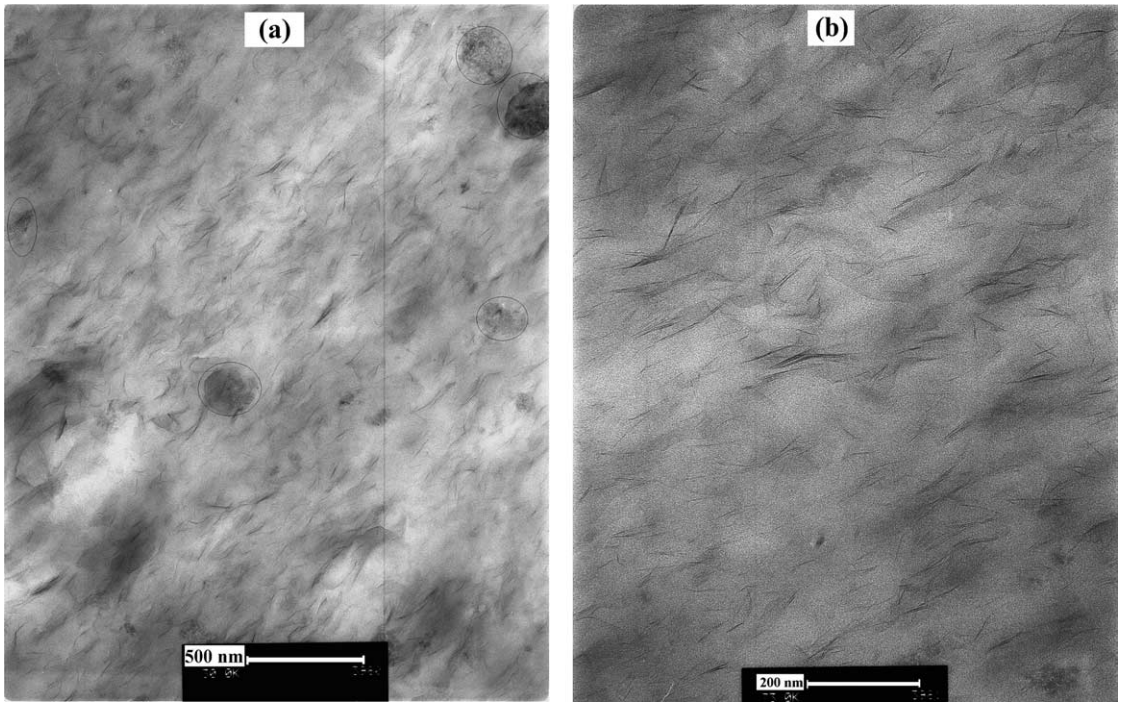

Fig. 5. Low and high magnification TEM image of PEA/PMMA–MMT (1.59%) nanocomposite.

We studied the thermal decomposition of PEA/PMMA and the corresponding nanocomposites as shown in Fig. 10. Unlike either PMMA–MMT or PEA–MMT systems [16,17], the main decomposition and end decomposition temperatures shift to higher values with increasing clay loading; however, the presence of clay does not affect the low temperature decomposition peak. We are still investigating this phenomenon.

4. Summary

Through a simple emulsion blending and heterocoagulation method, PEA/PMMA–MMT nanocomposites were prepared, which can be repeatedly processed without any discoloration. SAXS and TEM results confirmed the coexistence of exfoliated and intercalated structures; the homogeneously dispersed clay platelets in PEA/PMMA are parallel with the specimen surface.

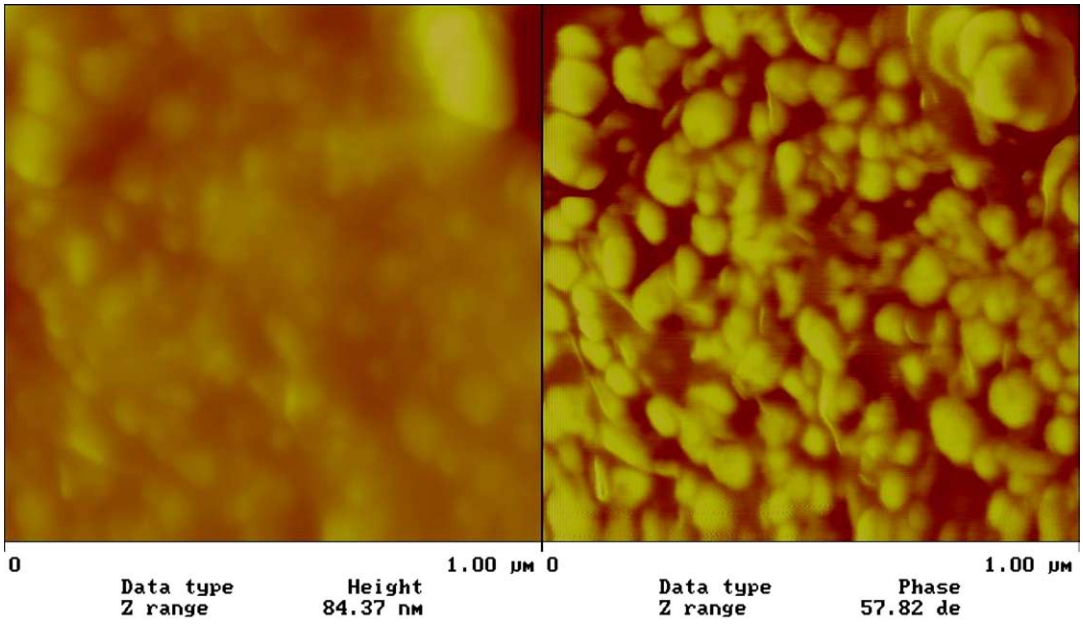

Fig. 6. AFM image of PEA/PMMA–MMT (1.59%) nanocomposite.

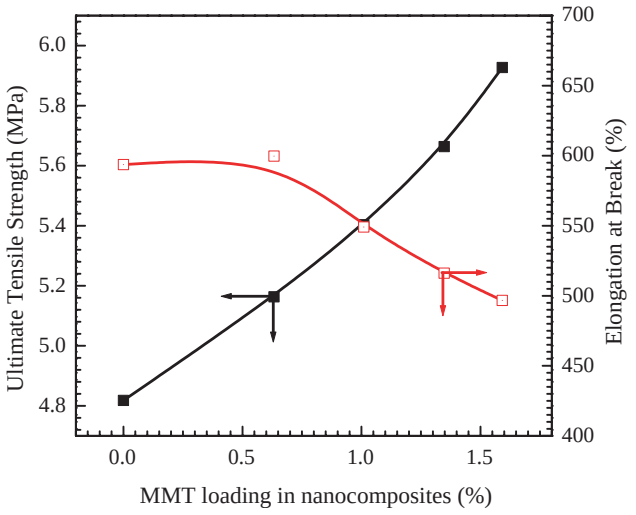

Fig. 7. Tensile stress and elongation at break of PEA/PMMA–MMT nanocomposite with respect to MMT loadings.

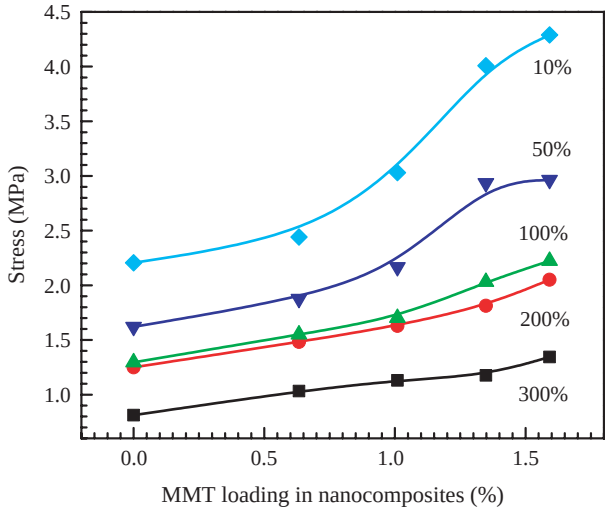

Fig. 8. Effect of MMT loading on stress–strain relationship of PEA/PMMA–MMT nanocomposites.

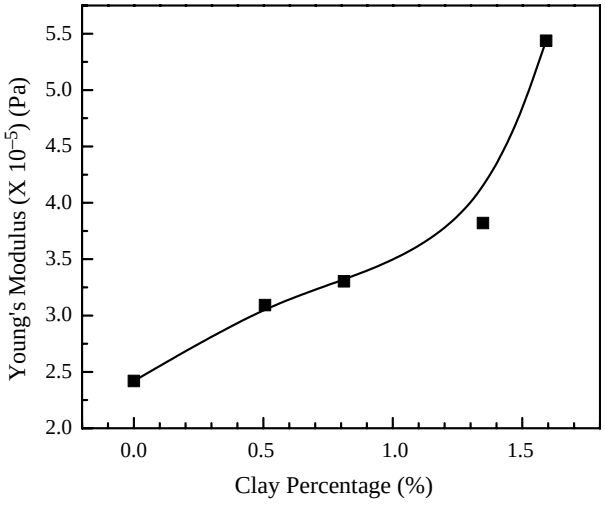

Fig. 9. Effect of MMT loading on the Young's modulus of PEA/PMMA–MMT nanocomposites.

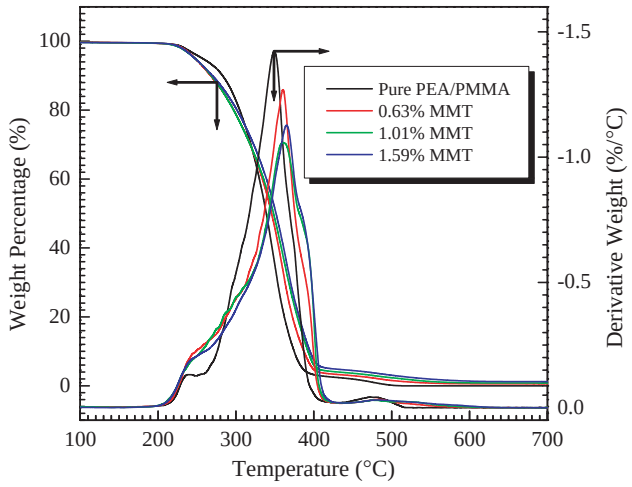

Fig. 10. Typical TG–DTG curves of pure PEA/PMMA blend and their nanocomposites.

AFM images suggested intimate contact of MMT platelets with both PMMA and PEA. The addition of MMT dramatically affected the mechanical properties of PEA/PMMA blends; with the addition of 1.59% MMT, the tensile strength increased by 23% and Young's modulus increased by 120%. DSC traces of the pure PEA/PMMA blends and their nanocomposites support a pressure-induced miscibility of PEA/PMMA system. TGA and DTG results indicated an improvement in main and end decomposition temperatures, but there is not effect on the suppression of the initial decomposition.

Acknowledgements

This research was supported by the DURINT on Microstructure, Processing and Mechanical Performance of Polymer Nanocomposites, Air Force Contract No. F49620-01-1-0447.

References

[1] Gonzalez-Leon JA, Acar MH, Ryu SW, Ruzette AVG, Mayes AM. Nature 2003;426:424.
[2] Pollard M, Russell TP, Ruzette AV, Mayes AM, Gallot Y. Macromolecules 1998;31:6493.
[3] Ruzette AVG, Banerjee P, Mayes AM, Russel TP. J Chem Phys 2001;114:8205.
[4] Ruzette AVG, Mayes AM, Pollard M, Russell TP, Hammouda B. Macromolecules 2003;36:3351.
[5] Ryu DY, Lee DJ, Kim JK, Lavery KA, Russell RP, Thiyagarajan P. Phys Rev Lett 2003;90:2335501.
[6] For recent reviews on preparation and properties of polymer–clay nanocomposites, see: Giannelis EP. Adv Mater 1996;8:29.
(b) Alexandre M, Dubois P. Mater Sci Eng 2000;28:1.
(c) Pinnavaia TJ, Beall GW, editors. Polymer–clay nanocomposites. Wiley: New York; 2000.
(d) Zilg C, Dietsche F, Hoffman B, Dietrich C, Mulhaupt R. Macromol Symp 2001;169:65.
(e) Vaia RA, Giannelis EP. MRS Bull; 2001:394.
(f) Schmidt D, Shah D, Giannelis EP. Curr Opin Solid State Mat Sci 2002;6:205.
[7] Fornes TD, Yoon PJ, Paul DR. Polymer 2003;44:7545.
[8] Xie W, Gao Z, Pan WP, Hunter D, Singh A, Vaia R. Chem Mater 2001;13:2979.

[9] Xie W, Gao Z, Liu K, Pan WP, Vaia R, Hunter D, et al. Thermochim Acta 2001;367–368:339.
[10] Zhu J, Uhl FM, Morgan AB, Wilkie CA. Chem Mater 2001;13:4649.
[11] Gilman JW, Awad WH, Davis RD, Shields J, Harris Jr RH, Davis C, et al. Chem Mater 2002;14:3776.
[12] Bottino FA, Fabbri E, Fragala IL, Malandrino G, Orestano A, Pilati F, et al. Macromol Rapid Commun 2003;24:1079.
[13] Hartwig PD, Schartel B, Bartholmai M, Wendschuh-Josties M. Macromol Chem Phys 2003;204:2247.
[14] Awad WH, Gilman JW, Nyden M, Harris Jr RH, Sutto TE, Callahan J, et al. Thermochim Acta 2004;409:3.
[15] Huang X, Brittain WJ. Macromolecules 2001;34:3255.
[16] Xu Y, Brittain WJ, Xue C, Eby RK. Polymer 2004;45:3735.
[17] Xu Y, Brittain WJ. J Appl Polym Sci 2006; in press.
[18] Mayes AM, Ruzette AV, Russell TP, Banerjee P. PCT WO01/60912A2.
[19] Cowie JMG, Ferguson R, Fernandez MD, Fernandez MJ, McEwen IJ. Macromolecules 1992;35:3170.
[20] Voulgaris D, Petridis D. Polymer 2002;43:2213.
[21] Wang Y, Zhang Q, Fu Q. Macromol Rapid Commun 2003;24:231.
[22] Wangale SD, Jog JP. J Appl Polym Sci 2003;90:3233.
[23] Laura DM, Keskkula H, Barlow JW, Paul DR. Polymer 2003;44:3347.
[24] Fornes TD, Paul DR. Macromolecules 2004;37:7698.